



Structure and temporal dynamics of the bacterial communities associated to microhabitats of the coral *Oculina patagonica*

Journal:	<i>Environmental Microbiology and Environmental Microbiology Reports</i>
Manuscript ID	Draft
Manuscript Type:	EMI - Research article
Journal:	Environmental Microbiology
Date Submitted by the Author:	n/a
Complete List of Authors:	Rubio-Portillo, Esther; Universidad de Alicante, División de Microbiología Santos, Fernando; Universidad de Alicante, División de Microbiología Martínez-García, Manuel; Universidad de Alicante, División de Microbiología; de los Rios, Asuncion Ascaso, Carmen; Museo Nacional de Ciencias Naturales, CSIC, Dept. Biología Ambiental Souza-Egipsy, Virginia; Instituto de Ciencias Agrarias, CSIC, Ramos-Esplá, Alfonso; University of Alicante Antón, Josefa; Universidad de Alicante, División de Microbiología
Keywords:	<i>Oculina patagonica</i> , Vibrio, Coral, Mucus, Holobiont, Bleaching, Microbiome

SCHOLARONE™
Manuscripts

1 A re-submission of **EMI-2016-0406**

2 **Structure and temporal dynamics of the bacterial communities associated**
3 **to microhabitats of the coral *Oculina patagonica***

4 Esther Rubio-Portillo^a, Fernando Santos^b, Manuel Martínez-García^b, Asunción de los Ríos^c,
5 Carmen Ascaso^c, Virginia Souza-Egipsy^d, Alfonso A. Ramos-Esplá^{a,e} and Josefa Anton^b

6 ^aDept. Marine Sciences and Applied Biology University of Alicante, 03080 Alicante, Spain

7 ^bDept. of Physiology, Genetics, and Microbiology, University of Alicante, 03080 Alicante,
8 Spain

9 ^cDept. Biogeochemistry and Microbial Ecology, Museo Nacional de Ciencias Naturales
10 (CSIC), 28006 Madrid, Spain

11 ^dInstituto Estructura de la Materia, (CSIC), 28006 Madrid, Spain.

12 ^eCentro de Investigación Marina (CIMAR), Universidad de Alicante-Ayuntamiento de
13 Santa Pola, Cabo de Santa Pola s/n, Alicante, Spain

14
15 **Originality-significance statement:** Corals are known to contain a diverse microbiota that
16 plays a paramount role in the physiology and health of holobiont. However, few studies
17 have addressed the variability of bacterial communities within the coral host. This is
18 precisely the central point of our work, which makes it different from previous
19 characterizations of coral microbiotas. We have characterized the bacterial community
20 composition from mucus, tissue and skeleton of the coral *Oculina patagonica*, seasonally
21 and at two locations in the Western Mediterranean Sea, to further understand how
22 environmental conditions and the coral microbiome structure are related.

23

24 **Abstract**

25 Corals are known to contain a diverse microbiota that plays a paramount role in the
26 physiology and health of holobiont. However, few studies have addressed the variability of
27 bacterial communities within the coral host. In this study, bacterial community composition
28 from the mucus, tissue and skeleton of the scleractinian coral *Oculina patagonica* were
29 investigated seasonally at two locations in the Western Mediterranean Sea, to further
30 understand how environmental conditions and the coral microbiome structure are related.
31 We used denaturing gradient gel electrophoresis in combination with next-generation
32 sequencing and electron microscopy to characterize the bacterial community. The bacterial
33 communities were significantly different among coral compartments, and coral tissue
34 displayed the greatest changes related to environmental conditions and coral health status.
35 Species belonging to the *Rhodobacteraceae* and *Vibrionaceae* families form part of *O.*
36 *patagonica* tissues core microbiome and may play significant roles in the nitrogen cycle.
37 Furthermore, sequences related to the coral pathogens, *Vibrio mediterranei* and *Vibrio*
38 *coralliilyticus*, were detected not only in bleached corals but also in healthy ones, even
39 during cold months. This fact opens a new view onto unveiling the role of pathogens in the
40 development of coral diseases in the future.

41

42

43

44

45

46

47

48 Introduction

49 Scleractinian corals form a collaborative consortium with a range of different microbial
50 partners: endosymbiotic dinoflagellates, bacteria, archaea, and viruses, which together form
51 the “coral holobiont” (Rohwer *et al.*, 2002; Knowlton and Rohwer, 2003). Unicellular
52 dinoflagellate algae from the genus *Symbiodinium* (Trench, 1979), also known as
53 zooxanthellae, are by far the best-understood microbial associate of corals. This mutualistic
54 symbiosis provides dinoflagellate photosynthetic products to the coral host, which
55 comprises up to 95% of coral energy requirements (Muscatine, 1990). Bacterial symbioses
56 are increasingly recognized as integral contributors to the coral holobiont, playing
57 significant roles in coral physiology and health (Rosenberg *et al.*, 2007; Wegley *et al.*,
58 2007, Kimes *et al.*, 2010; Bourne and Webster, 2013). Therefore, the coral holobiont is a
59 very rich consortium whose components interact in complex ways that are still very poorly
60 understood (Knowlton and Rohwer, 2003; Ainsworth *et al.*, 2010; Krediet *et al.*, 2013).

61 Corals have at least three different microhabitats (mucus, coral tissue and skeletal matrix)
62 with unique physicochemical characteristics and different bacterial communities (Sweet *et*
63 *al.*, 2011). Hence the understanding of coral-associated bacterial assemblages requires a
64 detailed knowledge of their distribution within the different coral compartments. The
65 interphase zones between the coral and its surrounding environment are constituted by the
66 surface mucus layer and the coral skeleton, which is a porous structure in contact not only
67 with seawater but also with sediments. In contrast, bacterial communities within the coral
68 tissues below the mucus are embedded in a more stable matrix and less exposed to
69 environmental changes, and therefore they may be less affected by variations in
70 environmental conditions.

71 There is some controversy in the literature regarding the influence of the environment on

72 coral-associated microbial communities. Some studies show that these communities are
73 coral-host specific across geographically distant sites (Rohwer *et al.*, 2002), suggesting that
74 the coral host determines the composition of prokaryotes within the holobiont. However,
75 more recent studies indicate that the influence of geographical and temporal factors in the
76 coral microbial composition is noteworthy (Hong *et al.*, 2009; Littman *et al.*, 2009; Barott
77 and Rohwer, 2012; Roder *et al.*, 2015).

78 Temperature can drive changes in host physiology and corals may suffer bleaching (corals
79 appear white because of the loss of their symbiotic zooxanthellae or their pigments, Brown,
80 1997) in response to elevated seawater temperatures (Hoegh-Guldberg, 1999; Hughes *et al.*,
81 2003). Not surprisingly, coral health status has a significant influence on the composition of
82 bacterial communities, which suffer changes during bleaching (Ritchie, 2006; Bourne *et al.*,
83 2008; Koren and Rosenberg, 2008). However, the role of these microorganisms in the
84 bleaching and whether their shifts are a cause or a consequence of this process are
85 uncertain.

86 Bleaching of the coral *Oculina patagonica* was first observed along the Israeli shoreline in
87 the summer of 1993 (Fine *et al.*, 2001) and it has been monitored since then (Israely *et al.*,
88 2001, Shenkar *et al.*, 2005). The *V. shiloi*-*O. patagonica* model system of coral bleaching
89 was studied intensively from 1996 to 2002 (reviewed by Rosenberg and Falkowitz, 2004).
90 The pathogen *Vibrio mediterranei* (= *Vibrio shilonii*) was also reported in 1996 as the
91 putative causative agent of the temperature-induced bleaching disease (Kushmaro *et al.*,
92 1996, 1997). Since 2002, the corals apparently became resistant to infection by *V.*
93 *mediterranei* (Reshef *et al.*, 2006) and a subsequent study stated that bacteria were not
94 directly involved in bleaching, but instead played a secondary role due to an increase of
95 susceptibility to microbial attack experienced by corals during environmental stress

96 (Ainsworth *et al.*, 2008). Recent studies (Mills *et al.*, 2013), including a study carried out
97 with the same coral samples analyzed in this work (Rubio-Portillo *et al.*, 2014a), suggested
98 that the coral pathogens *V. mediteranei* and *V. coralliilyticus* are indeed the causative agents
99 of bleaching in the coral *O. patagonica*.

100 It is well established that interactions among host-associated bacterial communities are
101 critical for the health of the coral holobiont (see revision by Krediet *et al.*, 2013), but our
102 limited knowledge about changes in resident microbiota associated with corals during non-
103 diseased states hinders the construction of an ecological model to explain what shifts in
104 coral microbiota are involved in coral diseases. Therefore, gaining knowledge about the
105 normal coral microbiota and how it changes over time is very important in order to
106 understand coral susceptibility to infection and its ability to survive bleaching.

107 The present study aims at describing the time-space variations of the microbial community
108 associated with the three different microhabitats (mucus layer, coral tissue and skeletal
109 matrix) present in the coral *O. patagonica*, which could have an influence on the coral
110 health status, by using a combination of microbiome profiling by Illumina sequencing and
111 DGGE of the 16S rRNA bacterial genes and transmission electron microscopy (TEM).
112 Overall, our results indicate that the bacterial communities are different among coral
113 microhabitats and that the coral tissue is the compartment whose microbiota best exhibit
114 changes under different environmental conditions. This finding contrasts with the fact that,
115 *a priori*, coral tissue would be expected to be steadier than the mucus or the skeletal matrix
116 since it is more isolated from the environment.

117 **Results and discussion**

118 Microbial cells were clearly observed in the in the mucus and tissue of *O. patagonica* by
119 transmission electron microscopy. Previously, our research group also detected by scanning

120 electron microscopy the presence of endolithic microorganisms in the skeletal matrix of *O.*
121 *patagonica* (Rubio-Portillo *et al.*, 2014b). Morphological diverse microbial aggregates were
122 observed in the mucus layer (Fig. 1A). At the epidermis and the tissue layer, bacteria with
123 coccoid and vibrio shapes are difficult to clearly differentiate from the abundant
124 cytoplasmatic inclusions. The presence of filamentous cell structures inside the
125 gastrodermal tissue was obvious in the samples collected in September 2011, during the
126 bleaching event, at the Harbor area (Fig. 1B and C).

127 In this work a total of 40 samples of *O. patagonica* taken from Alicante Harbor and the
128 Marine Protected Area (MPA) of Tabarca over a year, including a bleaching event on
129 September 2011, were used to monitor the bacterial communities from mucus, tissue and
130 skeleton compartments by DGGE analysis. A total of 12 gels were analyzed and 37
131 different bands were sequenced. Identification of band sequences was carried out using
132 BLASTn with the GenBank database (Table 2).

133 DNA from six different tissue samples were selected for sequencing using the Illumina
134 platform (see Experimental Procedures) and approximately 1.9 million reads were
135 generated. After removing short- and low-quality reads, as well as chimeras, a total of
136 562,494 sequences were obtained. The results related to the richness indexes, including
137 number of observed operational taxonomic units (OTUs) and Shannon's diversity indexes,
138 calculated as described in the Experimental Procedures, are summarized in Table 3. Most
139 of the samples contained up to 1,000 OTUs and the Shannon's indexes ranged from 5.72 to
140 8.28.

141 **Do different coral compartments harbor different bacterial communities?**

142 FPQuest analysis of the 16S rRNA PCR-DGGE amplicons from mucus, tissue and skeleton
143 of *O. patagonica* showed differences in bacterial diversity in the three compartments

144 (ANOVA, $p < 0.05$). Mucus (Shannon diversity index, $H' = 3.379$) and tissue ($H' = 3.305$)
145 harbored more diverse bacterial communities than skeletal matrix ($H' = 2.986$). The two-
146 dimensional NMDS plot (Fig. 2; stress value = 0.21) and cluster analysis (Fig. 2) also
147 showed that the bacterial composition was different among coral microhabitats (ANOSIM,
148 $R = 0.514$; $p = 0.001$), with the skeletal matrix harboring the most distinct bacterial
149 assemblage. This fact, together with the previous study carried out by Koren and Rosenberg
150 (2006) who observed different bacterial communities associated with mucus and tissues in
151 *O. patagonica*, confirmed the compartmentalization of bacterial communities within the *O.*
152 *patagonica* holobiont. This bacterial compartmentalization within the coral has also been
153 observed in the corals *Acroporapalmata* by Sweet *et al.* (2011) and in *Portiteslutea* (Li *et*
154 *al.*, 2014), using DGGE and pyrosequencing, respectively.

155 Most of the OTUs retrieved from mucus layer (61.50%) and coral tissue (61.11%) of *O.*
156 *patagonica* were classified as *Proteobacteria* (Fig. 3), with *Alphaproteobacteria* as the
157 dominant class of the microbial community in both microhabitats (84.89% and 64.8% of
158 *Proteobacteria*, respectively). *Gammaproteobacteria* were mainly detected in the tissue
159 compartment (22.52 % of tissue *Proteobacteria*), and *Deltaproteobacteria* in skeletal
160 matrix (33.91% of skeletal *Proteobacteria*). An analysis of contribution to similarities by
161 SIMPER was performed to determine which OTUs were primarily responsible for the
162 observed differences among the microhabitats studied (Supplementary Table 1). Data
163 indicated that *Ruegeria* (OTU AP3) and *Pseudovibrio* (OTU AP1) of the
164 *Rhodobacteraceae* family were identified (Supplementary Table 1) as important drivers of
165 these differences in the mucus layer, which were also relevant in the coral tissue layer
166 together with *Oceanicola* genus (OTU AP2). In the skeletal samples, OTU AP2 was the
167 most important together with a member of *Cytophaga* (BC1) that was found in 68% of the

168 skeletal samples.

169 Most of the OTUs retrieved from *O. patagonica* had high identities with members of
170 *Bacteria* previously detected in other marine invertebrates (see Table 2), such as sponges
171 and other coral species, even outside the Mediterranean Sea. This fact indicates that certain
172 members of the *O. patagonica* microbiota are shared with other marine invertebrates and
173 could be generalist symbionts displaying a broad host range and/or a widespread
174 occurrence.

175 DGGE analysis gels showed changes only in the coral tissue bacterial assemblages among
176 sampling time (Fig. 2) and coral health status (Fig. 4), while mucus and skeletal matrix
177 communities remained stable. For this reason, coral tissue samples from healthy and
178 bleached corals from the two localities during cold and warm months were also analyzed by
179 Illumina sequencing in order to obtain more information about bacterial assemblages and
180 the role of environmental conditions affecting coral holobiont health status.

181 **Comparison of bacterial communities associated with healthy and bleached tissues**

182 Many previous studies showed that microbial coral communities change during bleaching
183 events (Bourne *et al.*, 2008; Reis *et al.*, 2009; Lins-de-Barros *et al.*, 2013). In *O.*
184 *patagonica* tissues (Koren and Rosenberg, 2008) and other coral species the associated
185 bacterial diversity increases in diseased specimens (Bourne, 2005; Bourne *et al.*, 2008; Reis
186 *et al.*, 2009; Sunagawa *et al.*, 2009). Our results showed significant changes in bacterial
187 communities associated with bleached tissues (Fig. 4 and 5 for DGGE and Illumina results,
188 respectively), but diversity trends were different between localities. In corals from Alicante
189 Harbor, an increase in the bacterial diversity in bleached corals was observed, whereas in
190 the MPA, the highest bacterial diversity was detected in healthy corals (Table 3).

191 Bacterial communities associated to coral tissue from the Harbor and MPA collected in

192 warm months were more similar in bleached corals than in healthy ones (Fig. 4 and 5). As
193 both techniques used in this study indicated, a decrease of some OTUs belonging to
194 *Rhodobacteraceae* family was observed in healthy corals from both localities, specifically
195 of *Pseudovibrio* genus (Fig. 6 and Supplementary Table 1). Previous studies have
196 emphasized the possible role of *Pseudovibrio* species, detected in healthy tissues of corals
197 *Platygyracarous* in Hong Kong (Chiu *et al.*, 2012) and *Montrastreaannularis* in the
198 Florida Keys, as denitrifying heterotrophs in the nitrogen cycle of the coral holobiont
199 (Bondarev *et al.*, 2013), as well as their capacity to inhibit the growth of coral pathogens
200 (Nissimov *et al.*, 2009; Rypien *et al.*, 2010).

201 Even though the class *Gammaproteobacteria* was detected in both healthy and bleached
202 corals, their proportion was always higher in bleached corals, in which *Vibrio* genus
203 reached up to 60% of the Illumina reads. Among these sequences, those related to *V.*
204 *mediterranei* and *V. coralliilyticus*, two coral pathogens that promote *O. patagonica* coral
205 bleaching under aquaria conditions (Rubio-Portillo *et al.*, 2014a), were retrieved from both
206 healthy (including samples collected in cold months) and diseased corals (Fig. 7). Given the
207 low resolution of 16S rRNA gene partial sequences to identify *Vibrio* species (Thompson *et*
208 *al.*, 2009), caution must be exerted to avoid over-interpretation of these results, although
209 they are in agreement with our previous finding of *Vibrio* pathogens in otherwise healthy
210 corals that were exposed to high temperatures under aquaria conditions (Rubio-Portillo *et*
211 *al.*, 2014a) and that subsequently underwent bleaching. In fact, the sequences detected here
212 are more than 99% identical to the pathogens detected in these aquaria.

213 The detection of both *Vibrio* pathogens in healthy corals, even during cold months (0.01-
214 0.04 % of the total sequences), suggests that these pathogens could be in a viable but non
215 cultivable (VBNC) state inside coral tissues. The samples used in this study had been

216 analyzed by a culture dependent approach (Rubio-Portillo *et al.*, 2014a) that resulted in the
217 isolation of known vibrio pathogens only from diseased corals, which suggests that the
218 sequences detected here correspond to VBNC pathogens. This is in good agreement with
219 the results of Sharon and Rosenberg (2010), who found VBNC *Vibrio* spp. in the mucus
220 layer of *O. patagonica*. According to this hypothesis, the increase of seawater temperature
221 during warm months could trigger *O. patagonica* diseases through the activation of the
222 VBNC *Vibrio* communities associated to the coral tissue.

223 **The *O. patagonica* core microbiome and its predicted roles in healthy corals**

224 Analysis of the core microbiome of the coral *O. patagonica* from Illumina sequencing
225 demonstrated that only 14 of all bacterial OTUs identified were present in 100% of the
226 healthy corals (Table 4). Among these OTUs, most of them belonged to the
227 *Alphaproteobacteria* class, although *Vibrio* genus was also present in the core microbiome,
228 as we observed previously by culture analysis of the same coral samples (Rubio-Portillo *et*
229 *al.*, 2014a). In spite of the fact that PCRs with archaeal DGGE primers were always
230 negative in all samples (data not shown), archaeal sequences were recovered from tissue
231 samples sequenced by Illumina and ranged from 0.3 to 0.7% with the exception of one
232 sample that was about 15%. Furthermore, *Thaumarchaeota* sequences related to
233 *Nitrosopumilus* genus were present in 100% of healthy corals (Fig. 4) and were similar to
234 those found in previous studies (Lins-de-Barros *et al.*, 2010; 2013). Species from
235 *Nitrosopumilus* are capable of ammonia oxidation and they may play a relevant role in the
236 holobiont nitrogen cycle as observed previously in the ascidian *Cystodytes dellechiaiei*
237 (Martínez-García *et al.*, 2008).

238 Predictive metagenomic analysis (PICRUST; Langille *et al.*, 2013) was used to estimate the
239 functional roles of the OTUs obtained by QIIME analysis of Illumina tissue libraries. This

240 approach, based on Ainsworth *et al.* (2015), though rather speculative, could shed some
241 light on the putative metabolic functions encompassed by the coral tissue associated
242 microbiota detected here. This analysis suggested that ABC transporters, sugar transporters
243 and ion-couple transporters would be the three most abundant prokaryotic genes (Table 5)
244 in the *O. patagonica* core microbiome. Previous studies indicated that prokaryotic genes
245 related to transporters of sugars and ions were very abundant in coral tissues and could be
246 related to metabolic exchange between the coral host and bacterial microbiota (Ainsworth
247 *et al.*, 2015). Other key pathways linked to energy metabolism, such as the nitrogen cycle,
248 were also highly abundant in the *O. patagonica* core microbiome. As mentioned above, the
249 core microbiome included different bacteria such as *Pseudovibrio* species that could be
250 involved in the nitrogen cycle in corals. Furthermore, *Vibrio* species associated to *O.*
251 *patagonica* might have a positive effect on coral health by fixing nitrogen, as shown
252 previously for other corals species (Chimetto *et al.*, 2008).

253 **Seasonal changes of the *O. patagonica* microbiome**

254 The phylum *Proteobacteria* was always the dominant group in coral tissues and constituted
255 54 to 93% of the bacterial Illumina reads in coral tissues (Supplementary Figure 1). The
256 dominance of *Proteobacteria* in coral tissues has been observed previously in other studies
257 using both DGGE (Rohwer *et al.*, 2002; Littman *et al.*, 2009) and pyrosequencing
258 techniques (Wegley *et al.*, 2007; Pantos *et al.*, 2015). However, the relative proportion of
259 sequences belonging to different classes within the phylum changed depending on the
260 technique (Fig. 3 for DGGE and Supplementary 1 for Illumina), most likely due to the bias
261 exerted by different ribosomal operon copy numbers. For example, the number of
262 ribosomal operons in members of the *Vibrionaceae* and *Rhodobacteraceae* families varies
263 from 6 to 15, and 1 to 6, respectively (Stoddard *et al.*, 2014). Therefore, in the NGS

264 analysis, the abundance of sequences belonging to one given species could depend on its
265 ribosomal operon copy number and thus we may be detecting several sequences that belong
266 to the same organism, such as the case of *Vibrionaceae* family members.

267 In general terms, both techniques showed a decrease of *Alphaproteobacteria* class, mainly
268 the order *Rhodobacterales*, and an increase of *Gammaproteobacteria*, in particular
269 *Vibrionales* in *O. patagonica* tissues during warm months (Fig. 3 for DGGE and
270 Supplementary Figure 1b for Illumina), which was consistent with the results obtained by
271 Koren and Rosenberg (2006). Specifically, the OTUs belonging to the genus *Pseudovibrio*
272 (AP1 in DGGE and 19 and 20 in Illumina), as well as the order *Vibrionales* (GP2 in DGGE
273 and OTUs 37-51 in Illumina) were identified as the OTUs that mainly contributed to the
274 differences between samples taken in cold or warm months. Therefore, the microbiota in
275 the tissues of *O. patagonica* experience shifts during warm months that may have an effect
276 on coral health, either due to the decrease of *Pseudovibrio* representatives known to inhibit
277 the growth of coral pathogens, or to the direct increase of pathogenic *Vibrio* species. These
278 shifts are likely due to the increase of seawater temperature although other factors not
279 considered here could also be involved.

280 **Comparison among localities**

281 There was no clustering of the DGGE microhabitats samples by sampling location, and the
282 ANOSIM test confirmed that bacterial communities were not significantly different among
283 environments (Harbor and Tabarca, $R=0.019$; $p=0.710$). Differences between localities
284 were detected, however, in Illumina libraries as observed by UniFrac-based principal
285 coordinate analysis (Fig. 5), mainly due to the deeper resolution of the technique.
286 Consistent with our results, Lee *et al.* (2012) suggested that the sensitivity and resolution of
287 DGGE in revealing microbial diversity and community structure is probably lower than

288 NGS based 16S rRNA gene analysis, which allows for detecting differences among
289 bacterial communities associated with corals from sites with different environmental
290 conditions, including water nutrient content.

291 In Illumina tissue libraries, the Shannon's indexes were higher in the Harbor corals
292 (7.59 ± 0.76) than in the MPA (5.28 ± 0.36), at 0.03 cutoff. In both sampling locations the
293 bacterial community was dominated by the phylum *Proteobacteria*, but the class
294 *Gammaproteobacteria* showed a larger proportion in the Harbor than in Tabarca, where the
295 class *Alphaproteobacteria* was dominant. Hence, not only the diversity but also the
296 composition of the bacterial communities associated to *O. patagonica* differed substantially
297 from pristine to disturbed areas (previously characterized in terms of chlorophyll and
298 organic matter concentrations in Rubio-Portillo *et al.*, 2014c), which could also contribute
299 to differences in coral susceptibility to diseases. This is in agreement with previous findings
300 (Vezzulli *et al.*, 2013) that also reported higher bacterial diversity associated with the coral
301 *Paramuricea clavata* in Mediterranean locations affected by humans.

302 **Comparison of Illumina and DGGE to profile bacterial assemblages in *O. patagonica***

303 Although, overall, Illumina sequencing of 16S rRNA genes and PCR-DGGE have
304 considerable overlap in the main OTUs found in the *O. patagonica* core microbiome, there
305 were some differences regarding the bacterial composition they each revealed. Although
306 the primers used in both techniques match with similar percentages of classes belonging to
307 *Proteobacteriaphylum* gene sequences in the non-redundant Silva database (data not
308 shown), the presence of some minority classes (less than 5% of the sequences in Illumina
309 libraries), like *Betaproteobacteria* or *Epsilonproteobacteria*, was detected in *O. patagonica*
310 tissues solely by NGS analysis. The proportions of *Alphaproteobacteria* and
311 *Gammaproteobacteria* shown by each technique differed, probably due to the differences in

312 the number of ribosomal operons in both classes (see above). In any case, we should take
313 into account that neither of these techniques is suitable for quantification purposes since
314 both involve a PCR amplification step (Polz *et al.*, 1999). In fact, when four prokaryotic
315 species, *H. walsbyi*, *S. ruber*, *V. mediterranei* and *V. splendidus* were analyzed by DGGE
316 and Illumina 16S rRNA gene sequencing, both techniques failed at describing the actual
317 proportion of each species (Table 6). This fact confirms that DGGE band intensity should
318 not be used as a quantitative measure of relative abundance of organisms in environmental
319 samples as previously described (Murray *et al.*, 1996). This is to be expected since it
320 includes a 30-cycle PCR step. In addition, the ribosomal operon copy number may also
321 introduce a bias in an Illumina analysis, as discussed above. Thus, both techniques might be
322 calibrated by other methods like FISH or by metagenomic analyses, in which DNA is
323 sequenced without a prior amplification (Sharpton, 2014).

324 Therefore we can conclude that: i) OTUs belonging to the core microbiome with relative
325 abundance up to 1% (see Table 4) can be detected by DGGE and NGS, in agreement with
326 the detection threshold for DGGE (Muyzer *et al.*, 1993); ii) DGGE is a good technique to
327 describe differences among bacterial assemblages associated with the three different
328 compartments present in the coral holobiont, and is a suitable tool to check the similarity
329 among sample replicates; iii) Illumina 16S rRNA gene sequencing is better than DGGE to
330 detect rare taxa including coral pathogens or shifts in bacterial composition due to
331 environmental changes; and iv) neither of these two techniques is suitable to measure the
332 relative abundance of organisms in environmental samples. The combination of both
333 techniques provides a better picture of the coral holobiont than either technique on its own.

334

335

336 **Conclusions**

337 Here we have shown that 16S rRNA gene PCR-DGGE and Illumina sequencing approaches
338 are suitable for providing useful qualitative information about microbial communities
339 associated to corals and their time-space variations, as well as changes in microbiota related
340 to coral health status. The use of these techniques unveils high bacterial diversity within the
341 three microhabitats (i.e. mucus, tissue and skeleton) of the coral *O. patagonica*. Bacterial
342 communities appear strongly compartmentalized within the coral, with the tissue as the
343 compartment that best reflected changes in environmental factors such as seawater nutrient
344 concentration or temperature. Furthermore, our results suggest the presence of coral
345 pathogens within the tissues of healthy specimens as well as the detection within the coral
346 microbiota of bacteria typically present in other marine invertebrates. These findings,
347 together with the ongoing expansion of *O. patagonica* throughout the Mediterranean Sea
348 (Sartoretto *et al.*, 2008) could have significant implications for disease propagation in the
349 present global change scenario.

350

351 **Experimental procedures**

352 **Sample collection**

353 Five *O. patagonica* samples were seasonally collected (December 2010, February 2011,
354 June 2011 and September 2011, when a bleaching event was detected by Rubio-Portillo *et*
355 *al.* 2014c) at two locations: Alicante Harbor (38°20'11.1"N, 00°29'11.8"9W) and the
356 Marine Protected Area (MPA) of Tabarca (38°09'59"N, 0°28'56"W) on the Alicante coast,
357 South East of Spain (Western Mediterranean Sea), covering different environmental
358 conditions based on organic matter and chlorophyll concentration in seawater, as reported
359 previously by Rubio-Portillo *et al.* (2014c). A total of 40 coral colonies were analyzed in

360 this study (Table 1). The samples were immediately placed in plastic bags underwater and
361 transported to the laboratory in a cooler (within <2 h). The three different microhabitats
362 (mucus, coral tissue and skeletal matrix) were separated from coral fragments. Firstly coral
363 fragments were placed in 50-ml centrifuge tubes and centrifuged for 3 min at 2,675xg
364 twice, using new tubes each time, to remove the mucus. After centrifugation, the coral
365 pieces were crushed in sterile seawater with a mortar and pestle and, after allowing the
366 CaCO₃ skeleton to settle during 15 min, the tissue was removed from the supernatant
367 (Koren and Rosenberg 2006) and the skeleton was washed with sterile seawater in order to
368 eliminate any residual tissues. The coral health status was estimated by chlorophyll a
369 measurements obtained from coral tissues as previously described by Rubio-Portillo *et al.*,
370 (2014a).

371 **Microscopy analyses**

372 Three samples from each locality and each seasonal sampling time were processed for
373 Scanning Electron Microscopy (SEM) studies (see Rubio-Portillo *et al.*, 2014c). Coral
374 fragments were fixed (3% glutaraldehyde followed by 1% OsO₄), dehydrated in an ethanol
375 series, and embedded in LR-White acrylic resin. After polymerization, the blocks were cut
376 and finely polished. The fine-polished surfaces of the cross sections were carbon coated and
377 finally examined using a DMS 960 Zeiss SEM equipped with a four-diode, semiconductor
378 BSE detector. The microscope operating conditions were: 0° tilt angle, 35° X-ray take-off
379 angle, 15 kV acceleration potential, 15 mm working distance and 1–5 nA specimen current
380 range. After that, the SEM ultrastructural study areas of interest were removed from the
381 polished sample and embedded for transmission electron microscopy (TEM) study in LR-
382 White acrylic resin. In this study only TEM images are shown. Then ultrathin sections were
383 obtained and collected on formvar copper grids. Grids were contrasted with lead citrate

384 (Reynolds, 1963) and observed in a LEO 910 TEM (80KV) using a BioscanGatan 792
385 digital camera.

386 **DNA extraction and polymerase chain reaction amplification of 16S rRNA genes**

387 Coral mucus, tissue and skeletal samples were centrifuged at 9,300×g for 15 min, and
388 pellets were used for DNA extraction, using the UltraClean Soil DNA Kit (MoBio;
389 Carlsbad, CA) following the manufacturer's instructions for maximum yield. The extracted
390 genomic DNA was used for PCR amplifications of bacterial 16S rRNA genes by using the
391 specific bacterial primer 341f-GC (Muyzer *et al.*, 1993) and the reverse universal primer
392 907R (Muyzer *et al.*, 1993). Each PCR mixture contained 5 µl of 10x PCR reaction buffer
393 (Invitrogen), 2.5 µl of 50 mM MgCl₂, 1 µl 10 mM dNTP mixture, 1 µl of 10 µM of each
394 primer, 1 units of Taq polymerase, sterile MilliQ water up to 50 µl and 30 ng of the
395 extracted DNA. The PCR program was: 94°C for 5 min, 65°C for 1 min, 72°C for 3 min and
396 9 touchdown cycles of: 94°C for 1 min, 65°C (with a decreasing of 1°C in each cycle) for 1
397 min, 72°C for 3 min, followed by 20 cycles of: 94°C for 1 min, 55°C for 1 min, 72°C for 3
398 min (Muyzer *et al.*, 1993); a step at 72°C for 30 min was added to minimize double band
399 formation (Janse *et al.*, 2004). PCR products were diluted 10-fold and used as templates for
400 a five cycle reamplification in order to eliminate heteroduplexes (Thompson *et al.*, 2002).
401 Since DGGE band migration patterns of replicate corral tissue samples taken at the same
402 time did not show significant differences, six of them, three from Alicante Harbor and three
403 from Tabarca, (two of the three samples were healthy corals, one collected in February and
404 the other in June, and the third sample was a bleached coral collected in June) were selected
405 for massive sequencing of 16S rRNA gene amplicons to analyze in depth the bacterial
406 communities associated to *O. patagonica* coral tissues. (Table 1). The V3-V4 region of the
407 16S rRNA gene was amplified using the specific bacterial primers Bakt-341f and Bakt-805r

408 (Herlemann *et al.*, 2011) containing Illumina-specific adapter sequences. Each PCR mixture
409 contained 5 μ l of 10x PCR reaction buffer (Invitrogen), 1.5 μ l of 50 mM MgCl₂, 1 μ l 10
410 mM dNTP mixture, 1 μ l of 100 μ M of each primer, 1 units of Taq polymerase, 3 μ l of BSA
411 (New England BioLabs), sterile MilliQ water up to 50 μ l and 10 ng of DNA. The
412 amplification products were purified with the the GeneJET PCR purification kit
413 (Fermentas, EU), quantified using the Qubit Kit (Invitrogen), and the quality (integrity and
414 presence of a unique band) was confirmed by 1% agarose gel electrophoresis.

415 **Analysis of bacterial community composition by denaturing gradient gel**
416 **electrophoresis (DGGE)**

417 DGGE was performed by using the DCode System (Bio-Rad, Hercules, CA). PCR products
418 (500 ng) were separated by electrophoresis at 100 V during 16 h in a linear gradient from
419 40% to 60% (where 100% of denaturant consists of 7 M urea and 40% formamide) in a 6%
420 (w/v) polyacrylamide gel (acrylamide-bisacrylamide gel stock solution 37.5:1; Bio-Rad), in
421 1x TAE buffer (40 mM Tris, pH 8.0; 20 mM acetic acid; 1 mM EDTA). DGGE gels were
422 stained for 30 min with SYBR Green, visualized under UV light and photographed with a
423 Typhoon 9410 (Amersham Biosciences) system.

424 DGGE gel images were analyzed using the FPQuest Software Version 5.10 (Bio-Rad). In
425 order to compensate for gel-to-gel differences and external distortion due to
426 electrophoresis, the DGGE patterns were aligned and normalized using an external ladder,
427 made by PCR products from specific marine bacteria. Bands that were visible under UV
428 light were excised from DGGE gels using sterile scalpel blades and soaked overnight in 20
429 μ l of MilliQ water. Two μ l of each band were then reamplified with the same primer set
430 and checked again by DGGE to ascertain that they corresponded to single bands and to
431 confirm that the band of interest was isolated. PCR products were purified using the

432 GeneJET PCR purification kit (Fermentas, EU) and sequenced with primer 907R using an
433 ABI 3730xl sequencer (Applied Biosystems). Partial 16S rRNA gene sequences were
434 compared with reference sequences using the BLAST (Basic Local Alignment Search
435 Tool) software and the reference National Centre of Biotechnology Information database
436 (<http://www.ncbi.nlm.nih.gov/>). The band sequences are available from Genbank under
437 accession numbers KU936838-KU936871. Sequences of different bands were clustered
438 into OTUs at 98.7%, the threshold recommended as the best for the definition of members
439 of a species by Stackebrandt and Ebers (2006) similarity using RDP.

440 **Statistical analysis**

441 The presence/absence of OTUs in each sample, obtained from DGGE analysis, was used to
442 construct a binary matrix that represented the banding patterns, and multivariate analyses
443 were performed with a Primer 5 software package (Clarke and Gorley, 2001). A distance
444 matrix was constructed using Bray–Curtis similarity, and hierarchical clustering analysis
445 (CLUSTER) (similarity dendrogram) and non-metric multidimensional scaling (NMDS)
446 were used to explore groupings of the samples, since replicates of the same coral status
447 collected from the same locality at the same sampling time were grouped into the same plot
448 since there were no differences among them. Analyses of similarity (ANOSIM) was used to
449 determine if coral microhabitat (mucus/tissue/skeleton), sampling time (cold months:
450 December and February / warm months: June and September), coral status
451 (healthy/bleached), or sampling location (Harbor/Tabarca) had an effect on the bacterial
452 communities. Similarity percentage (SIMPER) was used to identify species that could be
453 potentially responsible for these differences.

454 **Illumina high-throughput 16S rRNA gene sequencing and bioinformatic analyses**

455 PCR products of the V3-V4 region were sequenced using a paired-end, 2×250-bp cycle run

456 on an IlluminaMiSeq sequencing system (Genomics Service at the Universidad Autónoma
457 de Barcelona, Spain) and raw reads were deposited in the NCBI Sequence Read Archive
458 (SRA) database under BioProject ID PRJNA315808. Downstream bioinformatic analyses
459 were performed using QIIME 1.8.0 (Caporaso *et al.*, 2010). Paired-end reads were assigned
460 to their respective samples according to their barcodes and then sequences were screened
461 by quality and size, and de-replicated with the script `split_libraries.py` (Caporaso *et al.*,
462 2010). Sequences were then subjected to the following procedures with QIIME scripts: (1)
463 chimeras were removed, (2) sequences were clustered at 97% similarity using UCLUST
464 (Edgar, 2010), (3) cluster representatives were selected, (4) SILVA_119 database (July
465 2014 edition) was used for taxonomic assignments of selected representatives by BLAST
466 and (5) tables with the abundance of different operational taxonomic units (OTUs) and their
467 taxonomic assignments in each sample were generated. Representative OTUs were also
468 aligned using PyNAST (Caporaso *et al.*, 2010) with the SILVA_119 database as a
469 reference. The number of reads was normalized to 6071 (the lowest number of the post-
470 assembly and filtered sequences in a sample) per sample. The number of OTUs and
471 Shannon diversity index values corresponding to 6071 sequences per sample were
472 calculated with QIIME. The similarity among different microbial communities was
473 assessed using phylogenetic information using jackknifed UPGMA (unweighted pair group
474 method with arithmetic mean) clustering based on the unweighted UniFrac (Lozupone and
475 Knight, 2005) distances between samples implemented in the QIIME pipeline. For
476 functional metagenome prediction, the PICRUST software package
477 (<http://picrust.github.com/picrust/>) (Langille *et al.*, 2013) was applied, which predicts the
478 gene content of a microbial community from the information inferred from 16S RNA genes
479 and using an existing database of microbial genomes which predicts the tentative function

480 of microbial communities. Metabolic predictions were made based on copy-number
481 normalized OTUs and using only healthy samples.

482 Sequences corresponding to the coral vibrio pathogens, *V. mediterranei* and *V.*
483 *coralliilyticus*, previously isolated from the same coral samples used in the present study
484 (Rubio-Portillo *et al.*, 2014a), were searched for in Illumina 16S rRNA gene libraries using
485 Basic Local Alignment Search Tool (BLAST 2.2.31+) with the following command ‘blastn
486 –perc_identity 98.7 –evalue 0.00001 –num_alignments 0 –maz_target_seqs 300000’.

487 **Comparison among DGGE and Illumina sequencing techniques**

488 In order to compare the results obtained by these two techniques, two controls of DNA
489 mixtures with different cell proportions were obtained from pure cultures of
490 *Haloquadratum walsbyi*, *Salinibacter ruber*, *Vibrio mediterranei* and *Vibrio splendidus*
491 (Table 6) with a known number of cells previously determined by 4'-6-diamidino-2-
492 phenylindole (DAPI) staining. These two controls were amplified with DGGE primers, and
493 electrophoresis was performed and stained as explained above. In parallel, the mock
494 communities were analyzed by Illumina sequencing as described above. DGGE band
495 intensities were quantified using PyElph 1.4 software and the relative contribution of
496 individual bands corresponding to each isolate to the total band intensity in the lane was
497 compared with the proportion of sequences obtained from Illumina sequencing of the same
498 DNA mixtures.

499 **Acknowledgments**

500 The authors gratefully thank the friendly cooperation of the Secretary-General for Fisheries
501 of the Spanish Ministry of Agriculture, Food and Environment, and of the Marine Reserve
502 of Tabarca guards (particularly Felio Lozano). We thank Karen Neller for her professional
503 text editing services. We are also grateful to the University of Alicante for awarding a pre-

504 doctorate grant to Esther Rubio-Portillo. This work was supported by the projects
505 CGL2012-39627-C03-01 and CGL2015-66686-C3-3-P (to JA) of the Spanish Ministry of
506 Economy and Competitiveness, that include FEDER funds from the European Union.

507 **References**

508 Ainsworth, T.D, Fine, M., Roff, G., Hoegh-Guldberg, O. (2008) Bacteria are not the
509 primary cause of bleaching in the Mediterranean coral *Oculina patagonica*. ISME J 2: 67–
510 73.

511 Ainsworth, T.D., Thurber, R.V., Gates, R.D. (2010) The future of coral reefs: a microbial
512 perspective. Trends Ecol Evol 25: 233–40.

513 Ainsworth, T. D., Krause, L., Bridge, T., Torda, G., Raina, J.-B., Zakrzewski, M., *et al.*
514 (2015) The coral core microbiome identifies rare bacterial taxa as ubiquitous
515 endosymbionts. ISME J 9:2261–2274

516 Barott, K., L., Rohwer, F.L. (2012) Unseen players shape benthic competition on coral
517 reefs. Trends in Microbiol 20: 621–8.

518 Bondarev, V., Richter, M., Romano, S., Piel, J., Schwedt, A., Schulz-Vogt, H. N. (2013)
519 The genus *Pseudovibrio* contains metabolically versatile bacteria adapted for symbiosis.
520 Environ Microbiol 15: 2095-2113.

521 Bourne, D.G. (2005) Microbiological assessment of a disease outbreak on corals from
522 Magnetic Island (Great Barrier Reef, Australia). Coral Reefs 24: 304–312

523 Bourne, D., Iida, Y., Uthicke, S., Smith-Keune, C. (2008) Changes in coral-associated
524 microbial communities during a bleaching event. ISME J 2: 350–363.

525 Bourne, D.G., Webster, N.S. (2013) Coral reef bacterial communities. In The Prokaryotes
526 (pp. 163-187). Springer Berlin Heidelberg.

527 Brown, B.E. (1997) Coral bleaching: causes and consequences. Coral Reefs 16:129-138.

- 528 Caporaso, J.G., Kuczynski, J., Stombaugh, J., Bittinger, K., Bushman, F.D., Costello, E., *et*
529 *al.* (2010) QIIME allows analysis of high-throughput community sequencing data. *Nat*
530 *Methods* 7: 335-336.
- 531 Chiu, J.M., Li, S., Li, A., Po, B., Zhang, R., Shin, P.K., Qiu, J. W. (2012). Bacteria
532 associated with skeletal tissue growth anomalies in the coral *Platygyracarnosus*. *FEMS*
533 *Microbiol Ecol* 79: 380-391.
- 534 Chimetto, L. A, Brocchi, M., Thompson, C. C., Martins, R. C. R., Ramos, H. R.,
535 Thompson, F. L. (2008) *Vibrios* dominate as culturable nitrogen-fixing bacteria of the
536 Brazilian coral *Mussismilia hispida*. *SystAppl Microbiol* 31: 312–319.
- 537 Clarke, K.R., Gorley, R.N. (2001) PRIMER version 5: user manual/tutorial. Primer-E Ltd,
538 Plymouth, UK, 91.
- 539 Edgar, R. C. (2010) Search and clustering orders of magnitude faster than BLAST.
540 *Bioinformatics* 26: 2460-2461.
- 541 Fine, M., Zibrowius, H., Loya, Y. (2001) *Oculina patagonica*: a non-lessepsian
542 scleractinian coral invading the Mediterranean Sea. *Mar Biol* 138: 1195-1203.
- 543 Herlemann, D.P., Labrenz, M., Jürgens, K., Bertilsson, S., Waniek, J.J., Andersson, A.F.
544 (2011) Transitions in bacterial communities along the 2000 km salinity gradient of the
545 Baltic Sea. *ISME J* 10: 1571-1579.
- 546 Hoegh-Guldberg, O. (1999) Climate change, coral bleaching and the future of the world's
547 coral reefs. *Mar Freshwater Res* 50: 839-866.
- 548 Hong, M.J., Yu, Y.T., Chen, C.A., Chiang, P.W., Tang, S. L. (2009) Influence of species
549 specificity and other factors on bacteria associated with the coral *Stylophora pistillata* in
550 Taiwan. *Appl Environ Microbiol* 75: 7797-7806.
- 551 Hughes, T.P., Baird, A.H., Bellwood, D.R., Card, M., Connolly, S. R., Folke, C., *et al.*

- 552 (2003) Climate change, human impacts, and the resilience of coral reefs. *Science* 301: 929-
553 933.
- 554 Israely, T., Banin, E., Rosenberg, E. (2001) Growth, differentiation and death of *Vibrio*
555 *shiloi* in coral tissue as a function of seawater temperature. *AquatMicrobEcol* 24: 1–8.
- 556 Janse, I., Bok, J., Zwart, G. (2004) A simple remedy against artifactual double bands in
557 denaturing gradient gel electrophoresis. *J Microbiol Methods* 57: 279–281
- 558 Kimes, N.E., Van Nostrand, J.D., Weil, E., Zhou, J., Morris, P.J. (2010) Microbial
559 functional structure of *Montastraea faveolata*, an important Caribbean reef- building coral,
560 differs between healthy and yellow-band diseased colonies. *Environ Microbiol* 12:541–556.
- 561 Knowlton, N., Rohwer, F. (2003) Multispecies microbial mutualisms on coral reefs: the
562 host as a habitat. *Am Nat* 162: 51- 62.
- 563 Koren, O., Rosenberg, E. (2006) Bacteria associated with mucus and tissues of the coral
564 *Oculina patagonica* in summer and winter. *Appl Environ Microbiol* 72: 5254–9.
- 565 Koren, O., Rosenberg, E. (2008) Bacteria associated with the bleached and cave coral
566 *Oculina patagonica*. *MicrobEcol* 55: 523–9.
- 567 Krediet, C.J., Ritchie, K.B., Paul, V.J., Teplitski, M. (2013) Promoting coral health and
568 thwarting diseases Coral-associated micro-organisms and their roles in promoting coral
569 health and thwarting diseases. *P Roy SocLond B Bio* 280: 20122328.
- 570 Kushmaro, A., Loya, Y., Fine, M., Rosenberg, E. (1996) Bacterial infection and coral
571 bleaching. *Nature* 380: 396.
- 572 Kushmaro, A., Rosenberg, E., Fine, M., Loya, Y. (1997) Bleaching of the coral *Oculina*
573 *patagonica* by *Vibrio* AK-1. *Mar EcolProgSer* 147: 159–165.
- 574 Langille, M.G.I., Zaneveld, J., Caporaso, J. G., McDonald, D., Knights, D., Reyes, J. *et al.*
575 (2013) Predictive functional profiling of microbial communities using 16S rRNA marker

- 576 gene sequences. *Nat Biotechnol* 31: 814–21.
- 577 Lee, O.O., Yang, J., Bougouffa, S., Wang, Y., Batang, Z., Tian, R., *et al.* (2012) Spatial and
578 species variations in bacterial communities associated with corals from the Red Sea as
579 revealed by pyrosequencing. *Appl Environ Microbiol* 78: 7173–84.
- 580 Li, J., Chen, Q., Long, L.J., Dong, J.-D., Yang, J., Zhang, S. (2014) Bacterial dynamics
581 within the mucus, tissue and skeleton of the coral *Poriteslutea* during different seasons. *Sci*
582 *Reports*, 4: 7320.
- 583 Lins-de-Barros, M.M., Vieira, R.P., Cardoso, A. M., Monteiro, V.A, Turque, A. S.,
584 Silveira, C. B., *et al.* (2010) Archaea, Bacteria, and algal plastids associated with the reef-
585 building corals *Siderastrea stellata* and *Mussismilia hispida* from Búzios, South Atlantic
586 Ocean, Brazil. *Microbial Ecol* 59: 523–32.
- 587 Lins-de-Barros, M.M., Cardoso, A.M., Silveira, C.B., Lima, J.L., Clementino, M.M.,
588 Martins, O.B., *et al.* (2013) Microbial Community Compositional Shifts in Bleached
589 Colonies of the Brazilian Reef-Building Coral *Siderastrea stellata*. *Microbial Ecol* 65:
590 205–13.
- 591 Littman, R.A., Willis, B.L., Pfeffer, C., Bourne, D.G. (2009) Diversities of coral-associated
592 bacteria differ with location, but not species, for three acroporid corals on the Great Barrier
593 Reef. *FEMS Microbiol Ecol* 68: 152–63.
- 594 Lozupone, C., Knight, R. (2005) UniFrac : a new phylogenetic method for comparing
595 microbial communities. *Appl Environ Microb* 71: 8228-8235.
- 596 Martínez-García, M., Stief, P., Díaz-Valdés, M., Wanner, G., Ramos-Esplá, A., Dubilier,
597 N., Antón, J. (2008) Ammonia-oxidizing Crenarchaeota and nitrification inside the tissue of
598 a colonial ascidian. *Environ microb*10 : 2991-3001.
- 599 Mills, E., Shechtman, K., Loya, Y., Rosenberg, E. (2013) Bacteria appear to play important

600 roles in both causing and preventing the bleaching of the coral *Oculina patagonica*. Mar
601 EcolProgSer 489: 155–162.

602 Murray, A. E., Hollibaugh, J. T., &Orrego, C. (1996). Phylogenetic compositions of
603 bacterioplankton from two California estuaries compared by denaturing gradient gel
604 electrophoresis of 16S rDNA fragments. Appl Environ Microbiol 62: 2676-2680.

605 Muscatine, L. (1990) The role of symbiotic algae in carbon and energy flux in reef corals.
606 In: Dubinsky, Z. (Ed.), Coral Reefs Ecosystems of the World. Elsevier, Amsterdam, pp.
607 75–87.

608 Muyzer, G., De Waal, E.C., Uitterlinden, A.G. (1993) Profiling in complex microbial
609 populations by denaturing gradient gel electrophoresis analysis of polymerase chain
610 reaction- amplified genes coding for 16S rRNA. Appl Environ Microbiol 59: 695–700.

611 Nissimov, J., Rosenberg, E., Munn, C. B. (2009) Antimicrobial properties of resident coral
612 mucus bacteria of *Oculina patagonica*. FEMS Microbiol Lett 292: 210–5

613 Pantos, O., Bongaerts, P., Dennis, P. G., Tyson, G. W., Hoegh-Guldberg, O. (2015)
614 Habitat-specific environmental conditions primarily control the microbiomes of the coral
615 *Seriatopora hystrix*. ISME J 9: 1916-1927.

616 Polz, M. F., Harbison, C., Cavanaugh, C. M. (1999). Diversity and heterogeneity of
617 epibiotic bacterial communities on the marine nematode *Eubostrichus diana*. Appl
618 Environ Microbiol 65: 4271-4275.

619 Reynolds, E.S. (1963) Use of lead citrate at high pH as an electron-opaque stain in electron
620 microscopy. J Cell Biol 17: 208-212.

621 Reis, A.M.M., Araujo, S.D., Moura, R. L., Francini, R.B., Pappas, G., Coelho, A.M.A., *et*
622 *al.* (2009) Bacterial diversity associated with the Brazilian endemic reef coral *Mussismilia*
623 *braziliensis*. J Appl Microbiol 106: 1378–1387.

- 624 Reshef, L., Koren, O., Loya, Y., Zilber-Rosenberg, I., Rosenberg, E. (2006) The coral
625 probiotic hypothesis. *Environ Microbiol* 8: 2068–2073.
- 626 Ritchie, K.B. (2006) Regulation of microbial populations by coral surface mucus and
627 mucus-associated bacteria. *Mar EcolProgSer* 322: 1–14.
- 628 Roder, C., Bayer, T., Aranda, M., Kruse, M., Voolstra, C. R. (2015) Microbiome structure
629 of the fungid coral *Ctenactisechinata* aligns with environmental differences. *MolEcol* 24:
630 3501-3511.
- 631 Rohwer, F., Seguritan, V., Azam, F., Knowlton, N. (2002) Diversity and distribution of
632 coral-associated bacteria. *Mar EcolProgSer* 243:1–10.
- 633 Rosenberg, E., Falkovitz, L. (2004) The *Vibrio shiloi/Oculina patagonica* model system of
634 coral bleaching. *Annu Rev Microbiol* 58: 143–59.
- 635 Rosenberg, E., Koren, O., Reshef, L., Efrony, R., Zilber-Rosenberg, I. (2007) The role of
636 microorganisms in coral health, disease and evolution. *Nat Rev. Microbiol* 5: 355–62.
- 637 Rubio-Portillo, E., Yarza, P., Peñalver, C., Ramos-Esplá, A.A., Antón, J. (2014a) New
638 insights into *Oculina patagonica* coral diseases and their associated *Vibrio* spp.
639 communities. *ISME J* 2003: 1–14.
- 640 Rubio-Portillo, E., Souza-Egipsy, V., Ascaso, C., De los Ríos, A., Ramos-Esplá, A.A.,
641 Antón, J. (2014b) Eukarya associated with the stony coral *Oculina patagonica* from the
642 Mediterranean Sea. *Mar Genomics* 17:17-23.
- 643 Rubio-Portillo, E., Vázquez-Luis, M., Valle, C., Izquierdo-Muñoz, A., Ramos-Esplá, A.A.
644 (2014c). Growth and bleaching of the coral *Oculina patagonica* under different
645 environmental conditions in the western Mediterranean Sea. *Mar Biol* 161: 2333-2343.
- 646 Rypien, K.L., Ward, J.R., Azam, F. (2010) Antagonistic interactions among coral-
647 associated bacteria. *Environ Microbiol* 12:28–39.

- 648 Sartoretto, S. (2008). The alien coral *Oculina patagonica* De Angelis, 1908 (Cnidaria,
649 Scleractinia) in Algeria and Tunisia. *Aquatic Invasions* 3: 173–180.
- 650 Sharon, G., Rosenberg, E. (2010) Healthy corals maintain *Vibrio* in the VBNC state.
651 *Environ Microbiol Rep* 2: 116–119.
- 652 Sharpton, T.J. (2014) An introduction to the analysis of shotgun metagenomic data. *Front*
653 *Plant Sci* 5:209.
- 654 Shenkar, N., Fine, M., Loya, Y. (2005) Size matters: bleaching dynamics of the coral
655 *Oculina patagonica*. *Mar Ecol Prog Ser* 294: 181–188.
- 656 Stackebrandt, E, Ebers, J. (2006) Taxonomic parameters revisited: tarnished gold standards.
657 *Microbiol Today* 8: 6–9.
- 658 Stoddard, S.F., Smith, B.J., Hein, R., Roller, B.R., Schmidt, T.M. (2015) rrnDB: improved
659 tools for interpreting rRNA gene abundance in bacteria and archaea and a new foundation
660 for future development. *Nucleic Acids Res*, D593-8.
- 661 Sunagawa, S., DeSantis, T.Z., Piceno, Y., Brodie, E., DeSalvo, M. K., Voolstra, C.R., *et al.*
662 (2009) Bacterial diversity and White Plague Disease-associated community changes in the
663 Caribbean coral *Montastraea faveolata*. *ISME J* 3:512–521.
- 664 Sweet, M.J., Croquer, A., Bythell, J.C. (2011) Bacterial assemblages differ between
665 compartments within the coral holobiont. *Coral Reefs* 30: 39-52.
- 666 Thompson, J.R, Marcelino, L.A, Polz, M.F. (2002) Heteroduplexes in mixed-template
667 amplifications: formation consequence and elimination by “reconditioning PCR”. *Nucleic*
668 *Acids Res* 30:2083-2088.
- 669 Thompson, C. C., Vicente, A. C. P., Souza, R. C., Vasconcelos, A. T. R., Vesth, T., Alves,
670 N., *et al.* (2009). Genomic taxonomy of vibrios. *BMC Evol Biol* 9: 258.
- 671 Trench, R.K. (1979) Cell biology of plant-animal symbiosis. *Annu Rev Plant Physiol Plant*

672 MolecBiol 30:485-531.

673 Vezzulli, L., Pezzati, E., Huete-Stauffer, C., Pruzzo, C., Cerrano, C. (2013) 16SrDNA

674 Pyrosequencing of the Mediterranean Gorgonian *Paramuricea clavata* reveals a link among

675 alterations in bacterial holobiont members, Anthropogenic Influence and Disease

676 Outbreaks. PloS One 8: e67745.

677 Wegley, L., Edwards, R.A., Rodriguez-Brito, B., Hong, L., Rohwer, F. (2007)

678 Metagenomic analysis of the microbial community associated with the coral *Porites*

679 *asteroides*. Environ Microbiol 9: 2707–2719.

680

681 **Figure legends**

682 Figure 1. Representative transmission electron micrographs of *Oculina patagonica* tissues

683 from September Harbor samples. A. Diverse morphological microbial cells from mucus

684 layer present in the external part of the coral. B. Filamentous bacteria (arrows) in the

685 gastrodermis in the area around mesoglea (M). C. The filamentous bacteria seem to

686 penetrate the coral tissue in an invasive way (arrows). Bars:1 μ m.

687 Harbor

688 Figure 2. Non-metric Multidimensional Scaling plots of the first two dimensions based on

689 Bray-Curtis dissimilarities for mucus (circles), tissue (squares), and skeletal matrix

690 (triangles), in gray samples collected in cold months (December and February) and in black

691 in warm months (June and September).

692 Figure 3. Cluster analysis and taxonomic composition (dominant bacterial sequence

693 affiliations grouped into dominant ribotypes at the class level) from DGGE analysis of only

694 healthy corals, with replicates grouped in the same plot, of mucus (M), tissue (T) and

695 skeletal (S) collected in cold (C) or warm (W) months from Alicante Harbor (H) or the

696 Marine Protected Area of Tabarca (T).

697 Figure 4. Non-metric Multidimensional Scaling plot, from all tissue profiles of DGGE, of
698 the first two dimensions based on Bray-Curtis dissimilarities. Alicante Harbor (circles) and
699 Marine Protected Area of Tabarca (squares), with black for healthy samples and white for
700 bleached ones.

701 Figure 5. Bacterial communities, detected by Illumina sequencing, associated to *Oculina*
702 *patagonica* tissues clustered using coordinated analysis of the weighed UniFrac distance
703 matrix. Each point corresponds to a coral sample from Alicante Harbor (circles) and Marine
704 Protected Area of Tabarca (squares), with black for healthy samples and white for diseased
705 ones. TCH: Tabarca Cold Healthy; TWH: Tabarca Warm Healthy; TWU: Tabarca Warm
706 Bleached; HCH: Harbor Cold Healthy; HWH: Harbor Warm Healthy; HWU: Harbor Warm
707 Bleached.

708 Figure 6. Heatmap summarizing the alpha diversity and abundance of the dominant
709 prokariotic OTUs, from Illumina analysis, (those present at more than 1% of abundance)
710 associated to *Oculina patagonica* tissues from Alicante Harbor and the Marine Protected
711 Area of Tabarca. TCH: Tabarca Cold Healthy; TWH: Tabarca Warm Healthy; TWU:
712 Tabarca Warm Bleached; HCH: Harbor Cold Healthy; HWH: Harbor Warm Healthy;
713 HWU: Harbor Warm Bleached.

714 Figure 7. Percentage of Illumina reads belonging to Vibrionacea genus and the percentage
715 of them that showed more than 98.7% of identity with *Vibrio mediterranei* and *Vibrio*
716 *coralliilyticus* sequences. See Table 3 for sample identifiers.

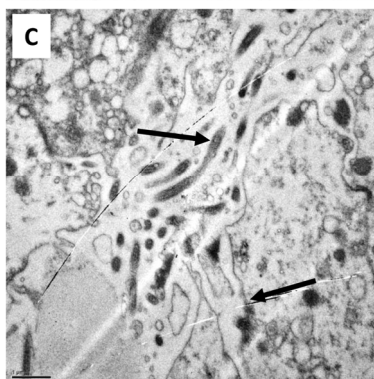
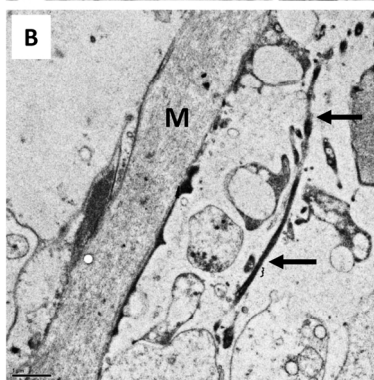
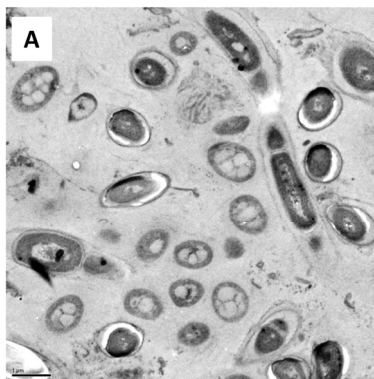
717 Supplementary Figure 1. Representative denaturing gradient gel electrophoresis (DGGE)
718 profiles of the coral tissue bacterial communities from samples collected in February in the
719 Alicante Harbor and the Marine Protected Area of Tabarca. Sequenced bands are marked

720 and named as Table 2. M: reference ladder.

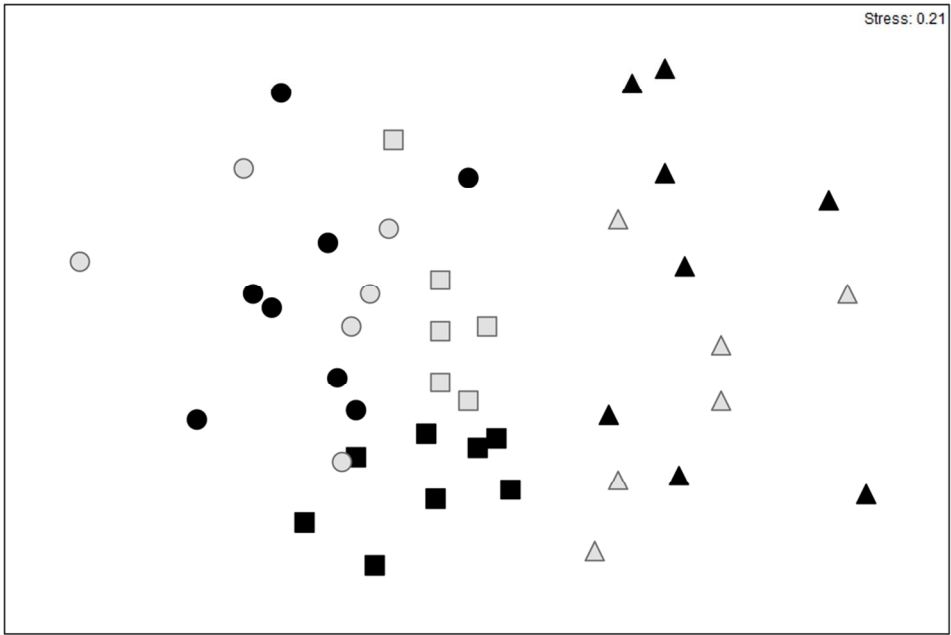
721 Supplementary Figure 2. Taxonomic classification of Illumina libraries into (a) phylum and

722 (b) class levels. See Table 3 for sample identifiers.

For Peer Review Only

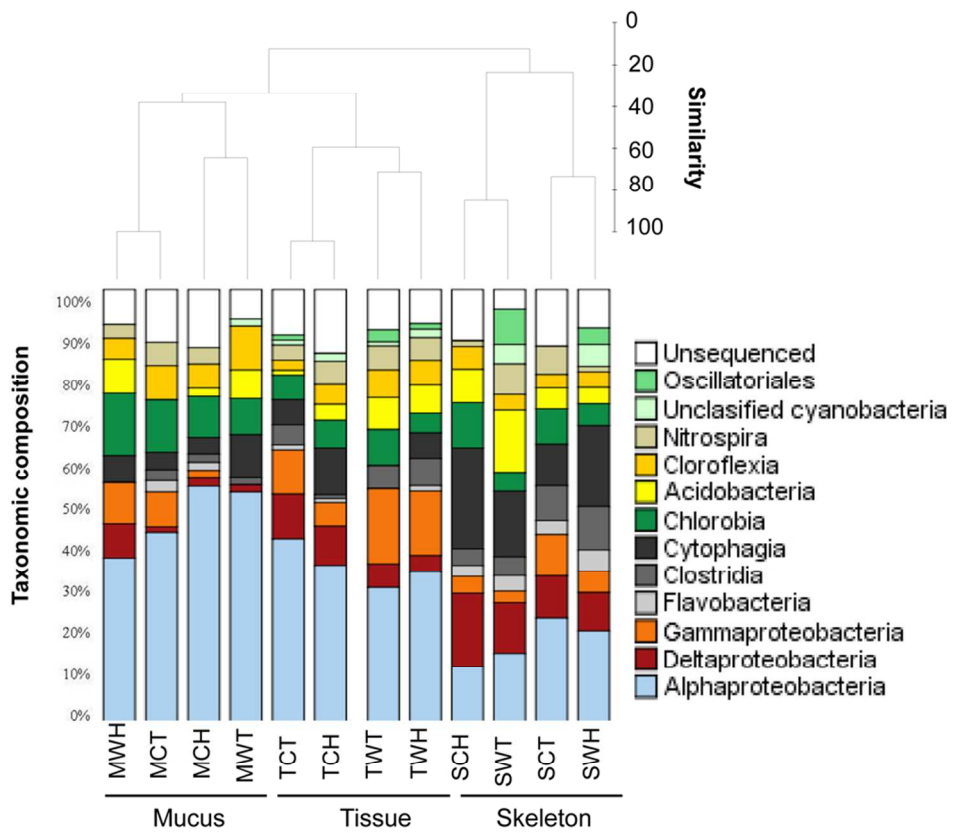


73x199mm (300 x 300 DPI)



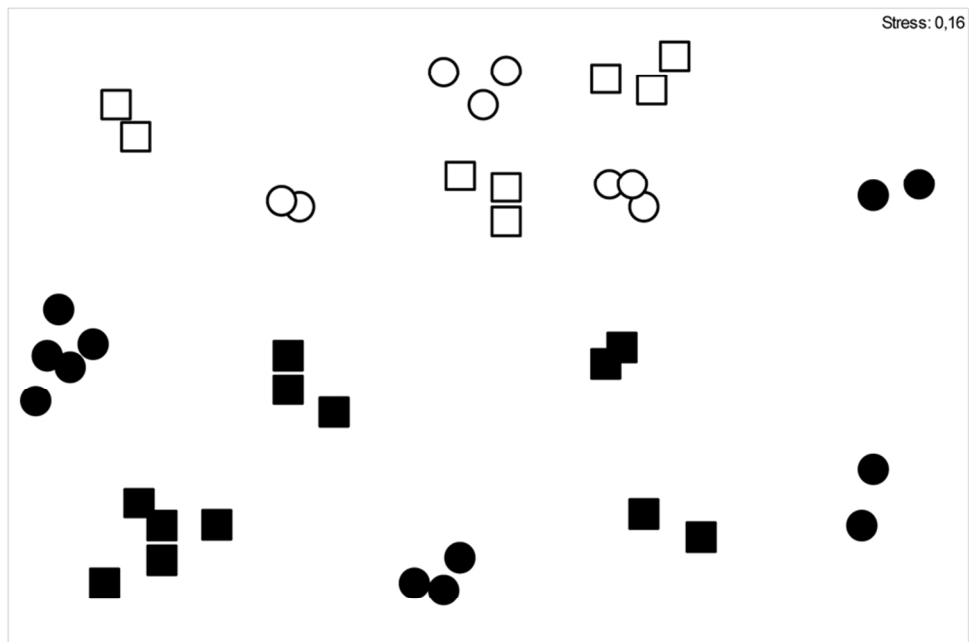
99x68mm (300 x 300 DPI)

View Only



90x77mm (300 x 300 DPI)

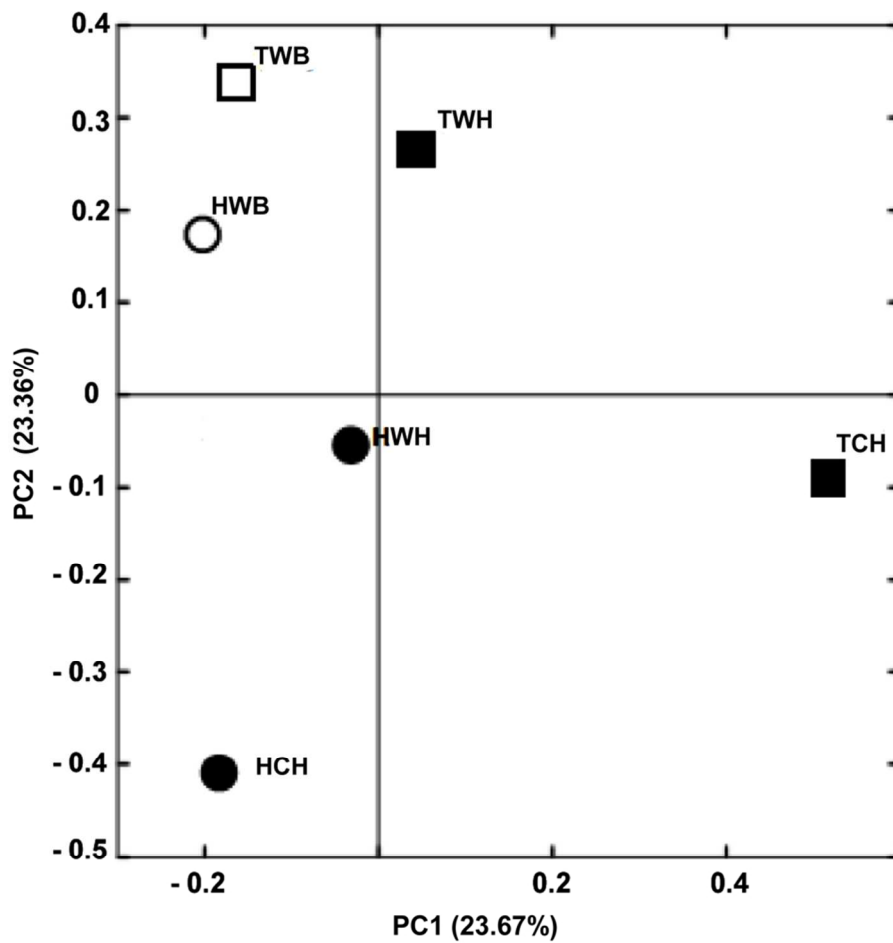
Only



- Harbour Bleached
- Tabarca Bleached
- Harbour Healthy
- Tabarca Healthy

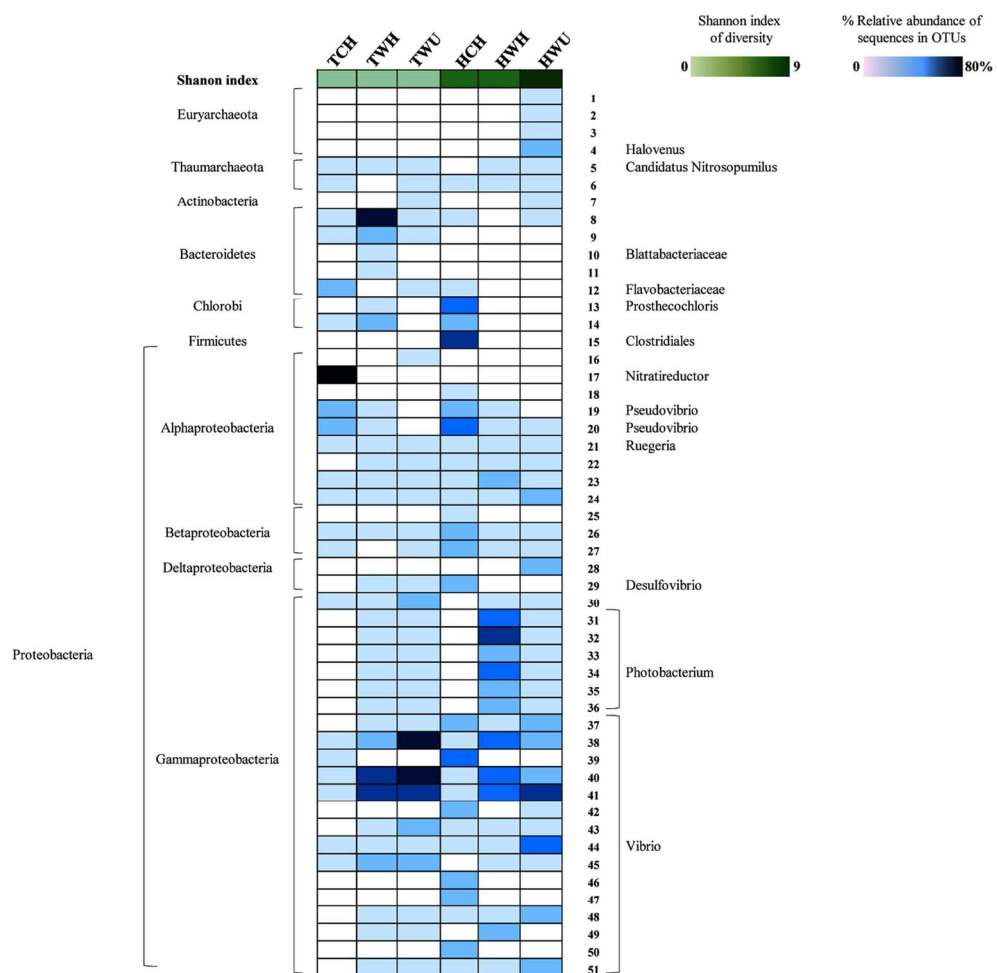
83x70mm (300 x 300 DPI)

Wiley-Blackwell and Society for Applied Microbiology



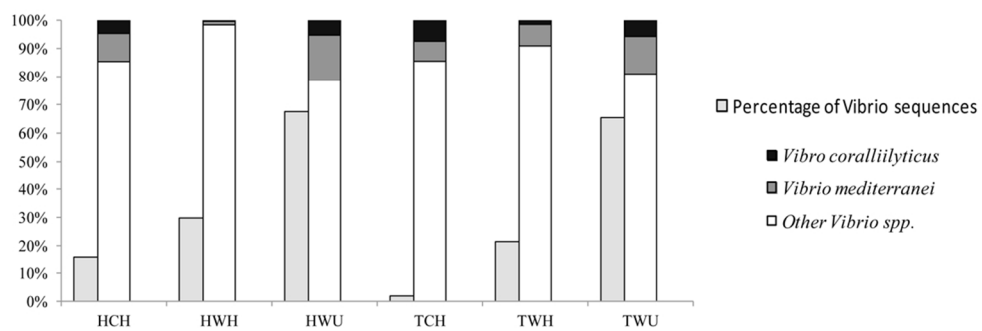
90x87mm (300 x 300 DPI)

only



140x141mm (300 x 300 DPI)





99x36mm (300 x 300 DPI)

Peer Review Only

Table 1. Summary of samples collected in this study.

Sampling Location	Sampling Time	Coral status	Replica	Techniques
Alicante Harbour	December 2010	Healthy	1-3	DGGE
		Bleached	4-5	DGGE
	February 2011	Healthy	1-4	DGGE
			5	DGGE and Illumina
	June 2011	Healthy	1-2	DGGE
		Bleached	3-5	DGGE
	September 2011	Healthy	1	DGGE and Illumina
			2	DGGE
		Bleached	3	DGGE and Illumina
			4 and 5	DGGE
MPA of Tabarca	December 2010	Healthy	1-3	DGGE
		Bleached	4-5	DGGE
	February 2011	Healthy	1-4	DGGE
			5	DGGE and Illumina
	June 2011	Healthy	1-2	DGGE
		Bleached	3-5	DGGE
	September 2011	Healthy	1	DGGE and Illumina
			2	DGGE
		Bleached	3	DGGE and Illumina
			4 and 5	DGGE

Table 2. Bacterial 16S rRNA sequences of selected DGGE bands.

OTU	Band	Sequence length (bp)	Phylogenetic group	Best hit in NCBI Source (% sequence identity, accession no.)	Closest type strain (% sequence identity, accession no.)
BC1	B1	513	Bacteroidetes (Cytophaga)	Uncultured Cytophaga Marine Sediments (88-89, AJ240979)	<i>Alkaliflexus imshenetskii</i> <i>Marinilabiliaceae</i> (86, AJ784993)
	B4	498			
	B6	531			
	B7	483			
BC2	B2	496	Bacteroidetes (Flavobacteria)	Uncultured Bacteroidetes bacterium Sponge-associated (99, AM259925)	<i>Vitellibacter aestuarii</i> (89, EU642844)
BC3	B3	318	Bacteroidetes (Cytophaga)	Uncultured Rhodothermaceae bacterium Sponge-associated (100, JQ612356)	<i>Rhodothermus profundus</i> (92, FJ624399)
BC4	B5	449	Bacteroidetes (Cytophaga)	Uncultured Cytophaga Hydrothermal vent chimney (97, FJ640814)	<i>Marivirga sericea</i> (92, AB078081)
BC5	B8	455	Bacteroidetes (Flavobacteria)	<i>Coralibacter albidofladus</i> Hard coral (99, AB377124)	<i>Pseudozobellia thermophila</i> (93, AB084261)
CB1	B9	493	Chlorobia	Prosthecochloris vibrioformis Marine aquaculture pond water (99, AM690798)	<i>Prosthecochloris vibrioformis</i> (98, M62791)
	B11	535			
CX1	B10	486	Chloroflexi	Uncultured bacterium Sponge-associated (98, FJ900573)	<i>Bellilinea caldifistulae</i> (81, AB243672)
	B14	406			
AB	B16	485	Acidobacteria	Uncultured bacterium KM3-173-A5 Mediterranean Sea (93, EU686629)	
AP1	B15	484	Alphaproteobacteria (Rhodobacterales)	<i>Pseudovibrio japonicus</i> Abalone	<i>Pseudovibrio japonicus</i> (100, AB246748)

	B23	493		(99, HE584768)	
	B18	466	Alphaproteobacteria (Rhodobacterales)	Rhodobacteraceae bacterium Coral-associated (99-100, JF411476)	<i>Pseudovibrio denitrificans</i> (99, AY486423)
	B19	512			
AP2	B17	522	Alphaproteobacteria (Rhodobacterales)	Uncultured bacterium Seawater (89, HQ203925)	<i>Oceanicola batsensis</i> (99, AY424898)
AP3	B20	516	Alphaproteobacteria (Rhodobacterales)	Uncultured bacterium Seawater (100, KC120680)	<i>Ruegeria atlantica</i> (99, D88526)
	B22	498			
	B21	498	Alphaproteobacteria (Rhodobacterales)	<i>Ruegeria sp.</i> JZ11ML32 Marine sponge (100, KC429919)	<i>Ruegeria conchae</i> (98, HQ171439)
	B24	493	Alphaproteobacteria (Rhodobacterales)	<i>Roseobacter sp.</i> 7m33 Soil (99, JQ66197)	<i>Ruegeria halocynthiae</i> (98, HQ852038)
AP4	B28	488	Alphaproteobacteria (Rhodospiralles)	Uncultured Alphaproteobacteria Sponge-associated (98, JF824774)	<i>Nisaea nitritireducens</i> (94, DQ665839)
DP1	B25	354	Deltaproteobacteria	Uncultured bacterium Marine sediments (99, EU488075)	<i>Sandaracinus amyolyticus</i> (92, HQ540311)
DP2	B35	488	Deltaproteobacteria	Uncultured microorganism Sponge-associated (100, JN002375)	<i>Desulfonatronum thiosulfatophilum</i> (85, FJ469578)
	B36	489			
GP1	B29	501	Gammaproteobacteria (Vibrionales)	<i>Photobacterium sp.</i> 1983 Phytoplankton culture (99, HF549205)	<i>Photobacterium frigidiphilum</i> (99, AY538749)
GP2	B30	380	Gammaproteobacteria (Vibrionales)	Vibrionales bacterium SWAT-3 (98%, AAZW01000075)	<i>Vibrio orientalis</i> (97, X74719)
	B31	455	Gammaproteobacteria (Vibrionales)	<i>Vibrio parahaemolyticus</i> (100, AAWQ1000319)	<i>Vibrio rotiferianus</i> (100, AJ316187)
GP3	B37	392	Gammaproteobacteria	<i>Psychrobacter glacincola</i>	<i>Psychrobacter piscatorii</i>

			(Pseudomonadales)	Sea ice (99, U85879)	(99, AB453700)
NI1	B26	498	Nitrospirae	Uncultured bacterium Sponge (99, EU035954)	<i>Nitrospira moscoviensis</i> (89, X822558)
FI1	B27	429	Firmicutes	<i>Clostridium sp.</i> AN-AS8 Sediments (97, FR872934)	<i>Defluviitalea saccharophila</i> (95, HQ020487)
CY1	B32	505	Cyanobacteria	<i>Oscillatroia corallinae</i> (99, X84812)	<i>Loriellopsis cavernicola</i> (93, HM748318)
CY2	B33	493	Cyanobacteria	Filamentous cyanobacterium Coral (96, EU196366)	<i>Prochlorothrix hollandica</i> (89, AM709625)

Table 3. Counts of paired-end rRNA gene sequences obtained from Illumina (preassembly) and following assembly and screened (postassembly) for the libraries included in this study. OTUS and Shannon diversity index were calculated from filtered sequences. H: Harbour; T: Tabarca; C: Cold; W: Warm; H: Healthy and B: Bleached

Samples	Location	Time	Coral Status	N° sequences		N° OTUS	Shannon diversity
				Preassembly	Postassembly and filtered		
HCH	Harbour	Cold	Healthy	3661044	222966	1779	7.75
HWH	Harbour	Warm	Healthy	126618	18268	1031	6.22
HWB	Harbour	Warm	Bleached	120202	15627	1748	8.19
TCH	Tabarca	Cold	Healthy	146276	275958	1537	5.33
TWH	Tabarca	Warm	Healthy	109296	6071	1005	5.68
TWB	Tabarca	Warm	Bleached	1396170	23604	1263	5.54

Table 4. Core microbiome community in *Oculina patagonica* (OTUs present in 100% of the samples analyzed by Illumina). Identity percentage indicates similarity to reference sequence used for taxonomic assignment. *: OTUs with more than 98% of identity with DGGE bands.

Silva Tag ID	Identity %	Taxonomic affiliation	Type strain (LTP database)	Identity %	Relative abundance based on Illumina sequences (Mean±SD)	Detected by DGGE
KF758600	99	Gammaproteobacteria; Vibrionales; Vibrionaceae; <i>Vibrio</i>	<i>Vibrio gigantis</i> (EF094888)	99	6.33 ± 4.19	*
ABXL01000053	99	Alphaproteobacteria; Rhodobacterales; Rhodobacteraceae; <i>Pseudovibrio</i>	<i>Pseudovibrio denitrificans</i> (AY486423)	99	3.02 ± 2.54	*
EU854926	99	Gammaproteobacteria; Vibrionales; Vibrionaceae; <i>Vibrio</i>	<i>Vibrio pelagius</i> (AJ293802)	99	2.32 ± 1.89	*
HE574865	99	Alphaproteobacteria; Rhodobacterales; Rhodobacteraceae; Uncultured bacterium	<i>Ruegeria conchae</i> (HQ171439)	99	1.17 ± 0.88	*
JF344078	99	Alphaproteobacteria; Rhodospirillales; Rhodospirillaceae; Uncultured bacterium	<i>Pelagibius litoralis</i> (DQ401091)	99	1.10 ± 1.1	*
EF629830	99	Alphaproteobacteria; Rhodobacterales; Rhodobacteraceae ; <i>Ruegeria</i>	<i>Ruegeria atlantica</i> (D88526)	99	0.84 ± 0.65	*
FR693291	99	Alphaproteobacteria; Rhodospirillales; Rhodospirillaceae; <i>Pelagibius</i>	<i>Pelagibius litoralis</i> (DQ401091)	95	0.82 ± 0.53	*
GQ140332	99	Betaproteobacteria; Burkholderiales; Comamonadaceae;	<i>Diaphorobacter nitroreducens</i> (AB064317)	98	0.53 ± 0.49	

		<i>Variovorax</i>				
JN606966	99	Gammaproteobacteria; Vibrionales; Vibrionaceae; <i>Vibrio</i>	<i>Vibrio crassostreae</i> (EF094887)	99	0.44 ± 0.31	
AY654819	99	Alphaproteobacteria; Rhodospirillales; Rhodospirillaceae	<i>Fodinicurvata halophila</i> (HG764424)	95	0.39 ± 0.37	
CU914838	99	Firmicutes; Clostridia; Clostridiales; Peptostreptococcaceae; <i>Tepidibacter</i>	<i>Tepidibacter mesophilus</i> (GQ231514)	98	0.06 ± 0.02	
JX411936	99	Gammaproteobacteria; Alteromonadales; Colwelliaceae; <i>Colwellia</i>	<i>Thalassomonas haliotis</i> (AB369381)	99	0.05 ± 0.03	
GQ906610	98	Archaea; Thaumarchaeota; Marine Group; Candidatus <i>Nitrosopumilus</i>	<i>Nitrososphaera viennensis</i> (CP007536)	95	0.05 ± 0.02	
EU236284	99	Alphaproteobacteria; Rhodobacterales; Rhodobacteraceae	<i>Roseovarius albus</i> (HF546052)	99	0.03 ± 0.02	

Table 5. Most abundant predicted KEGG pathways from the *Oculina patagonica* core microbiome using PICRUSt and copy-number normalized OTUs from healthy corals samples.

KEGG pathway	Possible function in symbiosis (based on Langille <i>et al.</i> , 2013)	Mean Abundance (% \pm SD)
Transporters	Transport of substrates (ions, sugars, lipids)	5.80 \pm 0.49
ABC transporters	Transport of substrates (ions, sugars, lipids)	3.87 \pm 0.23
Secretion systems	Secretion of proteins, including those involved in nutrient uptake	2.58 \pm 0.65
Other ion-coupled transporters	Transport of substrates (ions, sugars, lipids)	2.46 \pm 0.28
Purine metabolism	Nucleic acid metabolism	1.94 \pm 0.21
Pyrimidine metabolism	Nucleic acid metabolism	1.33 \pm 0.14
Ribosome	Genetic information processing	1.56 \pm 0.32
Oxidative phosphorylation	Energy metabolism	1.28 \pm 0.22
Nitrogen metabolism	Energy metabolism	1.18 \pm 0.29
Pyruvate metabolism	Energy metabolism	1.11 \pm 0.1

Table 6. Relative levels of isolates in control samples C1 and C2 as estimated by different molecular methods, including DGGE band intensity and proportion of sequences detected by Illumina sequencing.

Samples	Proportion of cells	% in DGGE analysis	% in Illumina library
C1			
<i>Salinibacter ruber</i>	48.9	57.84	35.3
<i>Haloquadratum walsbyi</i>	48.9	0	2.5
<i>Vibrio mediterranei</i>	2.1	22.93	16.3
<i>Vibrio splendidus</i>	0.1	18.01	45.8
C2			
<i>Salinibacter ruber</i>	25	21.22	9.09
<i>Haloquadratum walsbyi</i>	25	0	0.01
<i>Vibrio mediterranei</i>	25	50.58	85.5
<i>Vibrio splendidus</i>	25	28.22	5.3